Sensitivity to light weakly-coupled new physics at the precision frontier

Matthias Le Dall,[1] Maxim Pospelov,[1,2] and Adam Ritz[1]

[1] *Department of Physics and Astronomy, University of Victoria, Victoria, BC V8P 5C2, Canada*
[2] *Perimeter Institute for Theoretical Physics, Waterloo, ON N2J 2W9, Canada*

(Dated: May 2015)

Precision measurements of rare particle physics phenomena (flavor oscillations and decays, electric dipole moments, etc.) are often sensitive to the effects of new physics encoded in higher-dimensional operators with Wilson coefficients given by $\mathrm{C}/(\Lambda_{\rm NP})^n$, where C is dimensionless, $n \geq 1$, and $\Lambda_{\rm NP}$ is an energy scale. Many extensions of the Standard Model predict that $\Lambda_{\rm NP}$ should be at the electroweak scale or above, and the search for new short-distance physics is often stated as the primary goal of experiments at the precision frontier. In rather general terms, we investigate the alternative possibility: $\mathrm{C} \ll 1$, and $\Lambda_{\rm NP} \ll m_W$, to identify classes of precision measurements sensitive to light new physics (hidden sectors) that do not require an ultraviolet completion with additional states at or above the electroweak scale. We find that hadronic electric dipole moments, lepton number and flavor violation, non-universality, as well as lepton $g-2$ can be induced at interesting levels by hidden sectors with light degrees of freedom. In contrast, many hadronic flavor- and baryon number-violating observables, and precision probes of charged currents, typically require new physics with $\Lambda_{\rm NP} \gtrsim m_W$. Among the leptonic observables, we find that a non-zero electron electric dipole moment near the current level of sensitivity would point to the existence of new physics at or above the electroweak scale.

arXiv:1505.01865v3 [hep-ph] 9 Oct 2015

1. INTRODUCTION

Accelerator-based particle physics has the goal of probing the shortest distance scales directly, by colliding particles and their constituents at high energies. Thus far, all high energy data is well described by the Standard Model (SM) of particles and fields, with the last missing element, the Higgs boson, identified recently [1, 2]. Considerable attention is therefore focussed on the search for 'new physics' (NP) that may complement the SM by addressing some of its shortcomings. However, the most prominent empirical evidence for new physics, associated for example with neutrino mass and dark matter, does not necessarily point to an origin at shorter distance scales.

Fortunately, experiments at the energy frontier are not the only tools available to probe NP; they are supplemented by searches at the precision (and intensity) frontier (see *e.g.* [3]). Precision observables, particularly those that probe violations of exact or approximate symmetries of the Standard Model such as CP and flavor, play an important role in the search for new physics [4–7]. Their reach in energy scale, through loop-induced corrections from new UV physics, can often extend well beyond the direct reach of high energy colliders. However, measurements at low energies may be sensitive not only to NP corrections coming from the short distances, but also to NP at longer distances (lower mass) with extremely weak coupling to the SM. It is therefore prudent to ask for which precision observables can measured deviations from SM predictions *unambiguously* be identified with short-distance NP at the electroweak (EW) scale or above? Alternatively, one can ask when such deviations might also admit an interpretation in terms of new low-scale hidden sector degrees of freedom. This is the question we will address in this paper.

The sensitivity of any constraint on new physics is determined on one hand by the precision of the measurement in question, and on the other by the accuracy and precision of any SM calculations required to disentangle background contributions. If the effective Lagrangian is schematically written in the form $\mathcal{L} = \mathcal{L}_{\rm SM} + \mathcal{L}_{\rm NP}$, the possibility of discovery relies on being able to reliably bound the NP contribution to the observable away from zero. The natural tendency to interpret results in terms of operators in $\mathcal{L}_{\rm NP}$ induced by ultraviolet NP can be problematic, as $\mathcal{L}_{\rm NP}$ can in general also receive contributions from light weakly-coupled degrees of freedom. This dilemma is nicely illustrated by the theoretical interpretation of a NP discovery that has already occurred, namely the observation of neutrino flavor oscillations. The experimental results are most straightforwardly interpreted in terms of the masses and mixing of the light active neutrino species [8, 9]. However, as is well known, there are a number of possible explanations for their origin. These include a short-distance explanation in terms of the dimension-five Weinberg operator [10], $\mathcal{L}_{\rm NP} \propto (HL)(HL)/\Lambda_{\rm UV}$ with $\Lambda_{\rm UV} \gg \langle H \rangle$, which generates neutrino masses scaling as $\langle H \rangle^2/\Lambda_{\rm UV}$. There are also a variety of different UV completions for this operator, with and without heavy right-handed neutrino states, present throughout the theory literature. While this interpretation is certainly valid, there is also the possibility of interpreting neutrino mass as a consequence of very light states N, with $m_N \ll m_W$ and the quantum numbers of right-handed neutrinos [11–16]. Such states would typically be very weakly coupled to the SM, thus escaping direct detection. The most prominent model in this class is the simple three-generation extension of the SM with N states that allow Dirac masses for the active neutrinos. Thus we see that neutrino oscillations can be interpreted as the result of UV or IR new physics (or

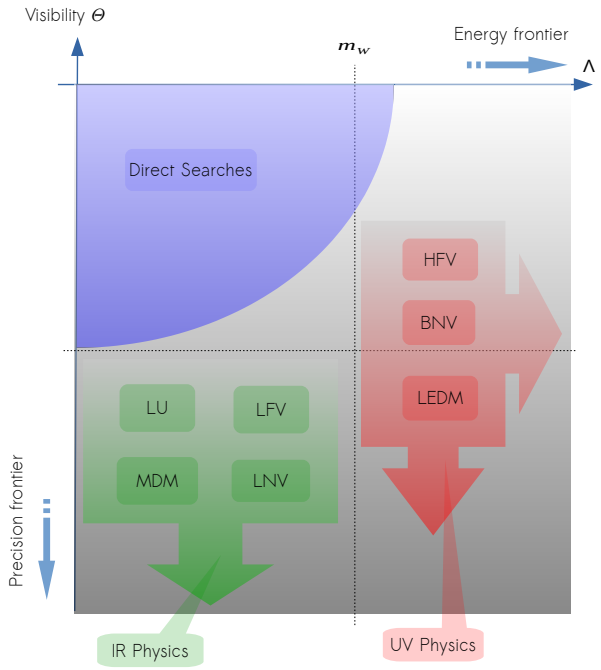

FIG. 1. A schematic view of the parameter space of mass scale vs coupling for physics beyond the SM. The horizontal axis represents the mass (or energy) scale, whereas the vertical scale shows the *visibility* of the model, in terms of the coupling to the SM. The blue visible area is accessible through direct searches. While new high energy physics can contribute to all precision observables, as discussed in this paper there are interesting classes of observables that are also sensitive to low-mass new physics. These are shown in green, and test lepton universality (LU), lepton flavor violation (LFV), lepton $g-2$ (MDM), and lepton number violation (LNV). However, observables in the hadronic sector in red, e.g. hadronic flavor violation (HFV) and baryon number violation (BNV), and also lepton electric dipole moments (LEDMs) generally require some new high scale physics. The arrows indicate the pressure imposed on models through increasing experimental sensitivity.

both).

In this paper we scrutinize several classes of precision frontier measurements, and confront them with the possibility of NP confined *solely* to low energy (sub-EW) scales. Our goal is to find specific examples of light NP that can induce CP-violation, cause deviations from calculated values of $g-2$, or lead to flavor changing effects. One condition we set on the classes of such models is the absence of any additional physics at or above the EW scale. In other words, we shall focus on UV complete models of light NP. Given the wealth of particle physics data, only very specific classes of light NP models can still be hidden below the weak scale. In Section 2, we describe this classification of infrared new physics scenarios in more detail. Then in Section 3 we discuss a number of different leptonic and hadronic observables, and explore simple new physics scenarios which provide a possible interpretation of any deviation in precision measurements. We summarize the analysis in Section 4. A schematic overview of the results is presented in Fig. 1, which illustrates the classes of (primarily leptonic) observables that can naturally be interpreted in terms of light UV-complete new physics.

2. UV AND IR NEW PHYSICS

A simple characterization of UV/IR new physics scenarios follows by making the division at the electroweak scale, so that the chiral electroweak $SU(2)_L \times U(1)_Y$ structure is maintained,

$$\mathcal{L}_{\rm NP} = \mathcal{L}_{\rm UV} + \mathcal{L}_{\rm IR}. \tag{1}$$

New UV physics can then universally be described at the EW scale by a series of higher dimensional operators constructed from SM degrees of freedom,

$$\mathcal{L}_{\rm UV} = \sum_{d\geq 5} \frac{1}{\Lambda_{\rm UV}^{d-4}} \mathcal{O}_d. \tag{2}$$

Maintaining SM gauge invariance explicitly, we demand that $\mathcal{O}_d$ can be written in an $SU(2)_L \times U(1)_Y$ covariant form. The lowest dimension $d=5$ includes only $LHLH$-type operators, which contribute to neutrino mass. The number of operators grows rapidly at $d=6$ and above [17]. We impose no restrictions on these operators, other than that $\Lambda_{\rm UV} \gg m_Z$, so that they can consistently be written in $SU(2)_L \times U(1)_Y$ covariant form. Unless these new operators violate some of the well-tested exact or approximate discrete symmetries of the SM, $\Lambda_{\rm UV}$ can be taken fairly close to the EW scale. It is important to notice that the new states appearing at $\Lambda_{\rm UV}$ could be charged under any of the SM gauge groups, and some of the most stringent constraints in cases where no specific symmetries are violated now come from the LHC.

In comparison, new IR physics is rather more constrained. A convenient categorization of light NP scenarios can be constructed as follows:

A. *Portals*: Neutral hidden sectors, with operators of dimension $d \leq 4$, can couple through a restricted set of renormalizable interaction channels, the vector, Higgs and neutrino portals (see e.g. [18]). Such models of light new physics are fully UV complete without any additional charged states.

B. *Anomaly free (neutral)*: Light hidden sectors can also be charged under anomaly-free combinations of SM symmetries. For those combinations, such as $B-L$ or $L_\mu - L_\tau$, that do not involve individual quark flavors, additional (light and neutral) Higgs fields may be necessary to retain a viable mass spectrum, but these extra states can be SM-neutral. Therefore, these scenarios also fall into the category of UV-complete and gauge-neutral hidden sectors.

C. *Anomaly free (charged)*: Light hidden sectors charged under anomaly-free, but quark-flavor non-universal, symmetries such as $Q_{f_1} - Q_{f_2}$ require new charged Higgs states to restore the mass spectrum. Thus, these new physics scenarios generally require charged states at or above the EW scale.

D. *Anomalous*: Light hidden sectors charged under anomalous SM symmetries, such as B or L, necessarily require additional (heavy) charged states at or above the EW scale, and so again do not fall into the category of IR new physics scenarios considered here. Indeed, as emphasized for example by Preskill [19], from the low energy perspective, anomalous theories are phenomenologically analogous to UV new physics scenarios with a specific UV cutoff.

Based on this categorization, we will limit our attention to cases A and B, namely those which do not require new charged states at or above the EW scale for consistency. Thus we construct our model examples according to the following rules:

- The dimensionality of operators in the IR sector is restricted to $d \leq 4$, as a necessary condition for UV completeness.
- The IR sector cannot contain new SM-charged states. (Otherwise, such states will have to be close to or above the EW scale modulo some exceptional cases where masses as low as ~ 60 GeV may still be viable [20]). New charged states fall into the category of NP at the EW scale, and form part of $\mathcal{L}_{\rm UV}$.
- The gauge extensions of the SM are restricted to anomaly-free combinations, which is also a generic requirement of UV completeness [19].
- We shall not question naturalness of possible mass hierarchies, $m_{\rm IR} \ll m_W$, and will take them as given.

The simplest type of neutral hidden sector (case A) requires new scalars S_i, neutral fermions N_i and/or new $U(1)$ gauge boson(s) V_μ [21]. The most economical renormalizable portal interactions for these states can be written in the form

$$\mathcal{L}_{\rm IR} = \kappa B^{\mu\nu} V_{\mu\nu} - H^\dagger H (AS + \lambda S^2) - Y_N L H N + \mathcal{L}_{\rm hid}, \quad (3)$$

and can trivially be generalized to multiple new fields and to a charged version of S, $S^2 \to |S|^2$. Once coupled to the SM through these channels, the IR hidden sector can be almost arbitrarily complicated. S and N can couple to a complex hidden sector involving dark abelian or non-abelian gauge groups, possibly with additional scalar or fermion states charged under those hidden gauge groups. The full hidden sector Lagrangian simply needs to comply with the conditions above. The portal interactions in (3) are complete under the assumption that the SM is strictly neutral under the extra $U(1)$. However, this is unnecessarily restrictive. Light NP models (in case B) may also include non-anomalous gauged versions of global symmetries such as $B - L$ and $L_i - L_j$ etc, where SM fields receive charges under the new $U(1)$.

It is also important to discuss some examples of theories that *do not* satisfy the above criteria. For example, a light pseudoscalar a coupled via the axion portal to a SM fermion ψ, $\frac{1}{f_a}\partial_\mu a\, \bar{\psi}\gamma^\mu\gamma_5\psi$, clearly requires UV completion at some high energy scale $\sim f_a$. Interestingly, a light scalar directly coupled to the scalar fermion density, $S\bar{\psi}\psi$, is allowed, provided that this coupling descends from the Higgs portal $ASH^\dagger H$, once the heavy SM Higgs particle is integrated out. This means, of course, that the ratio of the effective Yukawa couplings of S to ψ will obey the same relations as in the SM, and any deviations from this pattern would imply the existence of new Higgs doublets charged under the SM, and hence some new physics at or above the EW scale.

We turn in the next section to discuss a range of precision observables, and seek to determine which of them can receive significant contributions from IR new physics. Table 1 summarizes the results from the next section, and refines the schematic classification of Fig. 1 according to the categorization A–D of new physics models introduced above.

Observable	(A,B) Portals	(C,D) UV-incomplete
LFV	✓	✓
LU	✓	✓
$(g-2)_l$	✓	✓
LNV	✓	✓
LEDMs		✓
HFV		✓
BNV		✓

TABLE I. Observables sensitive to the distinct classes of light new physics models discussed in Section 2.

3. PRECISION OBSERVABLES

A. Lepton anomalous magnetic moments

The anomalous magnetic moments of the electron and the muon represent observables [22, 23] where the SM contribution can be evaluated to high accuracy. For electrons, the sensitivity to NP depends on an independent determination of the electromagnetic fine structure constant. Currently, $g-2$ of the electron (and related measurements) probe NP contributions at the level $\Delta a_e(\text{NP}) < 1.64 \times 10^{-12}$ (see *e.g.* [24]), whereas $g-2$ of the muon famously exhibits a roughly 3.5σ discrepancy [23] between the measurement and the SM prediction, with the central value giving $\Delta a_\mu \simeq 3 \times 10^{-9}$.

It is tempting to interpret this discrepancy as a consequence of NP that adds a positive contribution to the predicted SM value. While many UV interpretations exist (see *e.g.* [25]), Δa_μ(NP) can just as easily result from one-loop contributions of light particles. At the effective Lagrangian level, both $g' V_\nu \bar{\mu}\gamma^\nu \mu$ and $\lambda' S \bar{\mu}\mu$ can supply the requisite correction,

$$g', \lambda' \sim 10^{-3} \text{ with } m_{V(S)} \lesssim m_\mu \implies \Delta a_\mu \sim 10^{-9}. \quad (4)$$

This fact is well-appreciated in the literature [26–28].

The vector model has UV completions involving a kinetically mixed vector, or alternatively a symmetry based on gauged muon number, such as $L_\mu - L_\tau$. Dedicated searches for 'dark photons' [18] have now placed a number of restrictions on the parameter space of this model. At this point, the kinetically mixed vector option to explain $\Delta a_\mu \simeq 3 \times 10^{-9}$ is essentially ruled out through direct production experiments *assuming* V decays back primarily to SM states [29, 30]. Moreover, the alternative option of vectors decaying to light dark matter is also significantly constrained [31–33]. On the other hand, a model with mutliple (cascading) decays of V into the hidden sector can be ruled out only via missing energy signatures, and up to now, significant parameter space is still open for $\Delta a_\mu \sim O(10^{-9})$. The $L_\mu - L_\tau$ explanation is even less constrained, with only trident neutrino production providing an adequate level of sensitivity [34, 35]. We conclude that there are multiple IR models of NP that can lead to the observable shifts in $g-2$, while at the same time escaping direct detection constraints.

In contrast, models based on scalar particles do not provide large shifts to Δa_μ. For example, UV completion via Higgs mixing would imply

$$\lambda' \simeq \frac{A m_\mu}{m_h^2} \ll 10^{-3}, \quad (5)$$

as other constraints on the model force A to be much smaller than the weak scale, $A \ll m_h$. Thus, larger values of λ' would require additional NP to appear at the weak scale.

B. Lepton flavor violation and universality

We now turn to leptonic flavor-violating observables. In analyzing IR new physics scenarios, it will be convenient to have in mind a specific hidden sector coupled through the neutrino portal. In particular, to the three left-handed active neutrinos ν_l, $l = e, \mu, \tau$, we add corresponding right-handed neutrinos N_R, plus a number of extra singlet fermion states N_S. In our search for light NP models able to induce appreciable deviations of precision measurements in the lepton sector, it will prove advantageous to look in detail at a model that uses an inverse seesaw scheme for neutrino masses [36],

$$-\mathcal{L}_\nu \supset (\nu_L \quad N_R \quad N_S) \begin{pmatrix} 0 & m_D & 0 \\ m_D & 0 & M_D \\ 0 & M_D & \epsilon \end{pmatrix} \begin{pmatrix} \nu_L \\ N_R \\ N_S \end{pmatrix}, \quad (6)$$

in the regime $\epsilon \ll m_D, M_D$. The Dirac mass terms m_D, M_D are matrices, but in the simplest example of only one active flavor, one right-handed neutrino and one additional singlet, this model predicts one light and two heavy mass eigenstates, $m_\nu, M_\pm$ respectively, given by

$$m_\nu \sim \frac{m_D^2}{R^2}\epsilon + \mathcal{O}(\epsilon^2), \quad M_\pm \sim R \pm \frac{M_D^2}{2R^2}\epsilon + \mathcal{O}(\epsilon^2), \quad (7)$$

with $R^2 = m_D^2 + M_D^2$. In order to accommodate the light neutrino mass spectrum, we choose $m_D \lesssim M_D$, and $\epsilon \gtrsim m_\nu$. To lowest order, the unitary matrix U that transforms the mass eigenstates into the flavor eigenstates takes the form,

$$\begin{pmatrix} \nu_L \\ N_R \\ N_S \end{pmatrix} = U \begin{pmatrix} \nu_i \\ N_+ \\ N_- \end{pmatrix}, \quad U \approx \begin{pmatrix} \frac{M_D}{R} & \frac{m_D}{\sqrt{2}R} & i\frac{m_D}{\sqrt{2}R} \\ \frac{m_D M_D \epsilon}{R^3} & \frac{1}{\sqrt{2}} & -i\frac{1}{\sqrt{2}} \\ -\frac{m_D}{R} & \frac{M_D}{\sqrt{2}R} & i\frac{M_D}{\sqrt{2}R} \end{pmatrix}. \quad (8)$$

In the $m_D \ll M_D$ limit, the active neutrino states almost coincide with the flavor states $\nu_i \simeq \nu_l$, and the two singlets combine into heavy physical states $N_\pm \simeq (N_S \pm N_R)/\sqrt{2}$. The mixing between active-hidden and hidden-hidden neutrino states can also be measured by a set of three characteristic angles,

$$\theta_{\nu S} \approx \theta_{\nu N} \approx \frac{m_D}{\sqrt{2}M_D}, \quad \theta_{NS} \approx -\frac{\pi}{4} + \frac{m_D^2}{4M_D^2}. \quad (9)$$

Because the $\nu - S$ and $\nu - N$ mixing angles are so similar, we define the angle $\Theta_i \equiv \theta_{\nu_i N}$ to characterize the visible-hidden mixing.

We will generally make the assumption that the matrices M_D, ϵ are diagonal and universal, so that they are characterized by one scale also denoted M_D, ϵ respectively (this may involve some tuning, since in general it is not possible to simultaneously diagonalize both matrices). The visible Dirac masses m_D are nearly diagonal, but not universal, so that m_D can be characterized by three parameters $m_{De,\mu,\tau}$, thus $m_{\nu_l} \approx \epsilon m_{Dl}^2 / M_D^2$. The first two constraints on the model are those from the neutrino mass squared differences, $\Delta m_{21}^2 = m_{\nu_2}^2 - m_{\nu_1}^2$ and $\Delta m_{32}^2 = m_{\nu_3}^2 - m_{\nu_2}^2$,

$$\Theta_\mu^4 \simeq \frac{\Delta m_{21}^2}{4\epsilon^2} + \Theta_e^4, \quad \Theta_\tau^4 \simeq \frac{\Delta m_{32}^2 + \Delta m_{21}^2}{4\epsilon^2} + \Theta_e^4. \quad (10)$$

These functions have been plotted for clarity in Fig. 2. As we will see in the rest of this section, constraints can be imposed on Θ_e, cutting off some of the available parameter space. Further constraints could also be placed on $\Theta_{\mu,\tau}$, though we will not study these explicitly in this paper (see e.g. [37]).

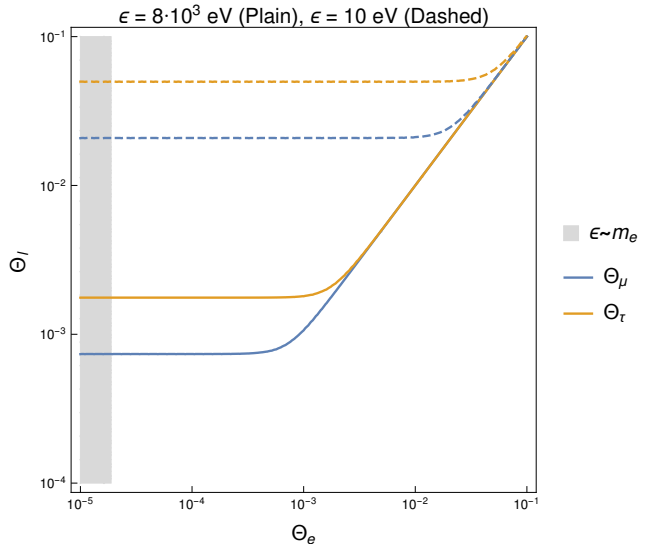

FIG. 2. A plot of the angles $\Theta_{\mu,\tau}$ given by equations (10), with $M_D = 3$ GeV. The gray band is inconsistent with the assumption that $\epsilon \ll m_D$.

B.1. Lepton flavor violation One NP-sensitive lepton flavor violating (LFV) observable is the $\mu \to e\gamma$ decay, whose branching ratio is experimentally constrained to satisfy $\mathrm{Br}(\mu^- \to e^-\gamma) < 5.7 \cdot 10^{-13}$ [38, 39]. The MEG-II upgrade is expected to have an order of magnitude better sensitivity [40]. Within the context of the SM, this process proceeds through a $W - \nu$ loop, an example of which is shown in Fig. 3. Including corrections from the massive neutrinos, the result is $\mathrm{Br}(\mu \to e\gamma) = (3\alpha/32\pi)\delta_\nu^2$ [41–45], with

$$\delta_\nu = 2 \sum_{i=\nu,\pm} U_{ei}^* U_{\mu i} g\left(\frac{m_i^2}{m_W^2}\right), \tag{11}$$

where

$$g(x) = \int_0^1 d\alpha \frac{1-\alpha}{1-\alpha+\alpha x}\left[2(1-\alpha)(2-\alpha)+\alpha(1+\alpha)x\right]. \tag{12}$$

In the small x limit, $g(x \ll 1) \approx 5/3 - x/2$, and using unitarity we find $\delta_\nu \approx -\sum_{i=\nu,\pm} U_{ei}^* U_{\mu i} m_i^2/m_W^2$. Furthermore, unitarity also implies $U_{e\nu}^* U_{\mu\nu} = -\sum_{i=\pm} U_{ei}^* U_{\mu i}$, resulting in a GIM-like dependence of δ_ν on the mass differences $m_\pm^2 - m_\nu^2$ [46]. Given the tiny active neutrino masses, the parameter δ_ν is dominated by the $M_\pm$ contributions $\delta_\nu \approx -\Theta_e\Theta_\mu(M_+^2 + M_-^2)/m_W^2$. Thus we have

$$\mathrm{Br}(\mu \to e\gamma) \approx \frac{3\alpha}{8\pi}\frac{M_D^4}{m_W^4}\Theta_e^2\Theta_\mu^2 < 5.7 \cdot 10^{-13}. \tag{13}$$

Inspection of this formula shows that there is ample room to saturate this inequality with light NP: taking $\Theta_e^2\Theta_\mu^2 \sim 10^{-8}$ and $M_D < m_W$ allows for $\mathrm{Br}(\mu \to e\gamma)$ at a level close to its upper bound.

For this particular light NP model, stronger sensitivity actually comes from $\mu - e$ conversion in nuclei [47–49]. There are two transition channels for this process.

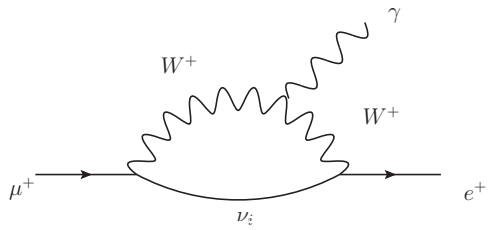

FIG. 3. Example of a $\mu \to e\gamma$ diagram.

First, the *photonic* transition, which proceeds via the same diagram as the $\mu \to e\gamma$ on-shell transition, except the photon is now connected to the nucleus. The second, the *non-photonic* transition, occurs either through Z-boson exchange or a box diagram mediated by W-bosons. Within the model considered here, the non-photonic transition is dominated by the box diagram. Since we focus on the light neutrino regime, we utilize the result that the box diagram receives a large enhancement (in this case) compared to the photonic transition, $\Gamma_{\not\gamma}/\Gamma_\gamma \sim 10^3$ [47], and the box diagram dominates the $\mu - e$ conversion rate. The conversion rate compared to muon capture in the nucleus, $R_{\mu-e} = \Gamma(\mu - e)/\Gamma_{capture}$, is given by

$$R_{\mu-e} \approx \left(\frac{3G_F m_W^2}{4\sqrt{2}\pi^2}\right)^2 \frac{E_e p_e}{m_\mu^2}|F_{ch}|^2 \rho \times \delta_\nu^2, \tag{14}$$

where

$$\rho \approx Z\frac{|3/2\beta_0(1+N/Z)+\beta_1/2(1-N/Z)|^2}{6|1.62Z/A-0.62|}, \tag{15}$$

is an enhancement factor accounting for the coherent nature of the transition. The charge form factor can be experimentally determined for various elements, the largest of which is about $|F_{ch}| \approx 0.5$ [49, 50]. The parameters $\beta_0 \sim 30$, $\beta_1 \sim 25$, and the factor $E_e p_e/m_\mu^2 \approx 1$. The best current limit is $R_{\mu-e} \leqslant 7.0 \cdot 10^{-13}$ from experiments using gold ^{197}Au [51], for which $Z = 79$, and the coherent enhancement factor is $\rho \approx 1.6 \cdot 10^6$. Therefore, using the above expression for δ_ν, we have

$$R_{\mu-e} \approx 6.5\delta_\nu^2 \approx 26\frac{M_D^4}{m_W^4}\Theta_e^2\Theta_\mu^2 \leqslant 7.0 \cdot 10^{-13}, \tag{16}$$

which is a stronger constraint on mass and mixing by two orders of magnitude than the $\mu \to e\gamma$ branching ratio. Various experiments, either running or in the planning stages, aim to increase sensitivity by several orders of magnitude [52, 53]. This inequality can again be saturated with $M_D \ll m_W$.

B.2. Lepton Universality Tests of lepton universality provide valuable constraints on masses and mixings of massive neutrinos. There exist various standard decay channels to test lepton universality (see *e.g.* [45, 54, 55]).

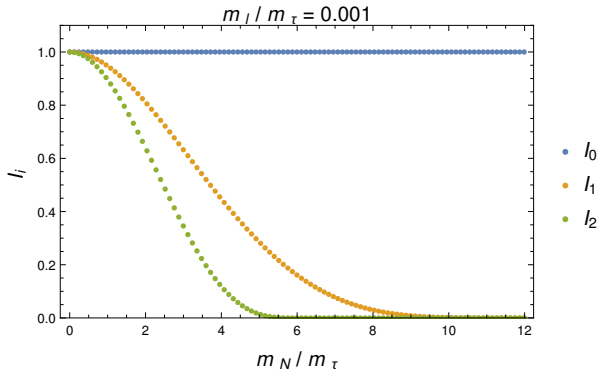

FIG. 4. Phase space factors $I_{0,1,2}$ for the $\tau \to l\nu\nu$ decay.

In particular, we will focus on $\mu - e$ universality in τ decays, through the R_τ observable defined as

$$R_\tau = \frac{\Gamma(\tau^- \to e^- \nu\nu)}{\Gamma(\tau^- \to \mu^- \nu\nu)}. \tag{17}$$

In the SM, because the neutrinos are massless, the flavor eigenstates ν_l and mass eigenstates ν_i coincide so that $\Gamma(\tau^- \to e^- \nu\nu) = \Gamma(\tau^- \to e^- \nu_\tau \nu_l)$. For massive neutrinos, and multiple neutrino states, the masses are linear combinations of flavor eigenstates, and $\Gamma(\tau^- \to e^- \nu\nu) = \sum_{i,j} \Gamma(\tau^- \to l^- \nu_i \nu_j)$. The R_τ ratio has recently been measured by BaBar, $R_\tau = 0.9796 \pm 0.0016 \pm 0.0036$ [56], which we will approximate as $R_\tau \approx 1 \pm \Delta R_\tau$, with $\Delta R_\tau = 0.0052$. In general, the decay rate takes the form [57, 58],

$$\Gamma(\tau^- \to l^- \nu\nu) = \frac{G_F^2 m_\tau^5}{192\pi^2} \sum_{ij} |U_{\tau i}|^2 |U_{lj}|^2 I\left(\frac{m_l^2}{m_\tau^2}, \frac{m_{\nu_{i,j}}^2}{m_\tau^2}\right). \tag{18}$$

To a good approximation, we can take the active neutrino masses to vanish, and the splitting between the two sterile neutrino states to be negligible, $M_+ - M_- \sim \epsilon \ll m_\tau$. Thus, the kinematic function I splits into three categories, where either zero, one or two of the sterile states are produced, respectively denoted $I_{0,1,2}$, with each depending only on the mass scales, but not the flavors. These are plotted in Fig. 4, and are very insensitive to the outgoing lepton masses m_μ and m_e. As a result,

$$\begin{aligned}\Gamma(\tau^- \to l^- \nu\nu) \propto I_0^l \sum_{i,j} |U_{\tau\nu_i}|^2 |U_{l\nu_j}|^2 + I_2^l \sum_{i,j} |U_{\tau N_i}|^2 |U_{lN_j}|^2 \\ + I_1^l \sum_{i,j} \left(|U_{\tau N_i}|^2 |U_{l\nu_j}|^2 + |U_{\tau\nu_i}|^2 |U_{lN_j}|^2\right).\end{aligned} \tag{19}$$

Using unitarity, we express the visible-visible mixing as $\sum_j |U_{l\nu_j}|^2 = 1 - \sum_i |U_{lN_i}|^2 \approx 1 - N_h \Theta_l^2$, using the assumption $U_{lN_i} = \Theta_l$, with N_h the number of hidden flavors. This approximation is valid as long as $1 - N_h \Theta_l^2 > 0$. The constraint comes from requiring that $\Delta R_\tau = 1 - \Gamma(\tau \to \mu\nu\nu)/\Gamma(\tau \to e\nu\nu) < 0.0052$ be within the experimental errors.

The actual significance of this constraint depends on the concrete realization of the mass and mixing pattern. For example, in the situation where the heavy neutrino eigenstates cannot be kinematically produced, the final constraint can be presented as $N_h |\Theta_\mu^2 - \Theta_e^2| < 10^{-2}$. A somewhat stronger universality constraint can be derived by comparing charged pion decay modes. These constraints can be saturated with $\Theta_l^2 \sim O(10^{-2})$ and, as we saw above, such a mixing pattern can easily arise from new singlet neutrino states with a mass below the electroweak scale.

In summary, using the neutrino mass differences to express $\Theta_{\mu,\tau}$ as functions of ϵ, Θ_e, we can present the LFV and universality constraints above in the parameter plots shown in Fig. 5. It is clear that this simple light NP model, with sub-EW scale singlet fermionic states, can induce deviations in $\mu \to e$ conversion or lepton universality at the level of the current experimental sensitivity. Therefore, if future experiments detect a non-zero result, further work will be required to unambiguously differentiate between light and heavy NP models.

C. Lepton number violation

Neutrinoless double beta decay $\beta\beta_{0\nu}$ is the primary observable for lepton number (L) violation, and the current limits [60–65] are normally interpreted directly in terms of the light neutrino mass spectrum [66, 67]. Given the existing mass limits on the light eigenstates, the decay rate depends on the effective Majorana mass $m_\nu^{\rm eff} = \sum_i U_{ei}^2 m_i$. Even without performing a dedicated analysis, it is clear that any future evidence for a non-zero $m_\nu^{\rm eff}$ will not be able to differentiate between light and heavy NP models. Indeed, in the simplest Type I see-saw model, $m_\nu^{\rm eff} \sim \mathcal{O}(\text{eV})$ can arise from models with *e.g.* $M_R \sim 1$ GeV or $M_R \sim 10^{10}$ GeV, and therefore both interpretations would be possible.

In what follows, for completeness, we analyze lepton number violation utilizing the same neutrino model as in the previous section. Recall that the heavy mass eigenstates N_i mix with ν_e, so that the mass eigenstates can be written as $N_i = U_{ei}\nu_e + \cdots$. It will be sufficient to work with the following analytic approximation for the decay rate [68],

$$\Gamma(\beta\beta_{0\nu}) \sim \frac{G_F^4 Q^5 \cos^4\theta_C}{60\pi^3} |\mathcal{M}|^2, \tag{20}$$

where $Q + M(Z, A) - M(Z+1, A)$ is the endpoint energy,

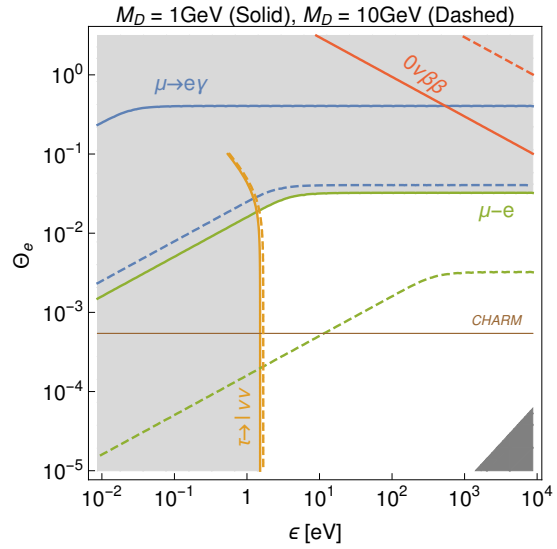

(a)

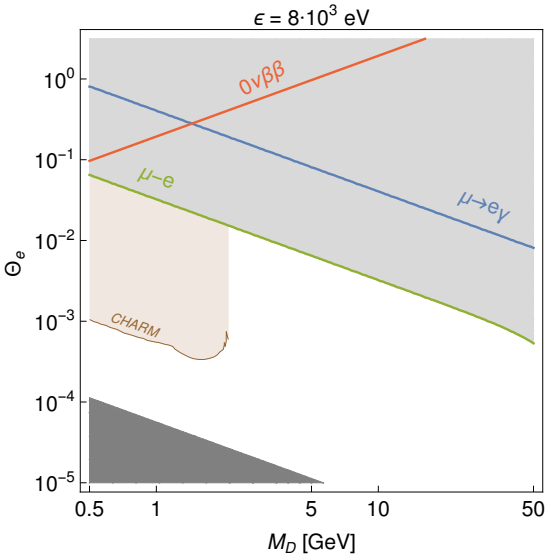

(b)

FIG. 5. Plots showing the allowed regions in (a) $\{\epsilon, \Theta_e\}$ and (b) $\{M_D, \Theta_e\}$ respectively, with $N_h = 2$. The lines correspond to saturation of the respective bounds. M_D is bounded above by the requirement $M_D < m_W$, and from below by the $0\nu\beta\beta$ constraint $M_D \gg 0.1$ GeV. We note that at large ϵ, the $\mu - e$ conversion constraint is by far the strongest, though universality becomes stronger at low ϵ. The darker gray area represents the regime where $\epsilon/m_e > 10^{-1}$, with ϵ no longer 'small'. For completeness, we also show a constraint from on-shell production of sterile states at the CHARM fixed target experiment [59], which applies for $M_D \lesssim 2\,\text{GeV}$.

and the amplitude takes the approximate form,

$$\mathcal{M} = \sum_i U_{ei}^2 m_i \int \frac{d^4p}{(2\pi)^4} \left(\frac{w(p_0, |\vec{p}|)}{p^2 - m_i^2 + i\epsilon} \right) \longrightarrow \frac{iE_F p_F w_0}{4\pi^3} \begin{cases} m_\nu^{\text{eff}} + \cdots & \text{for } p_F \gg m_i, \\ \frac{p_F^2}{3} \sum_i \frac{U_{ei}^2}{m_i} + \cdots & \text{for } p_F \ll m_i. \end{cases} \tag{21}$$

The nuclear form factor $w(p_0, |\vec{p}|)$ has been approximated by a step function $w \sim w_0 \Theta(p_0 - E_F)\Theta(|\vec{p}| - p_F)$, with $w_0 \sim 4$ MeV^{-1} [68] in terms of the nucleon Fermi momentum $p_F \sim 100$ MeV. (A more precise interpolating formula is given in [69].)

When the dominant contribution is from the light active neutrinos, the experimental bounds translate to $m_\nu^{\text{eff}} \lesssim 0.12\text{–}0.38$eV [62, 63]. It is also instructive to separately estimate the sensitivity to the exchange of heavier neutrino eigenstates. Note that when the singlet mass $m_N \gg p_F$, the experimental constraints lead to a bound on $(p_F^2/3)\sum_i U_{ei}^2/m_i$ instead. Within the neutrino mass model described in the previous section, we find

$$\sum_i \frac{U_{ei}^2}{m_i} \simeq \frac{U_{e+}^2}{M_+} + \frac{U_{e-}^2}{M_-} \simeq \Theta_e^2 \left(\frac{M_- - M_+}{M_+ M_-} \right), \tag{22}$$

where $M_- - M_+ \simeq -\epsilon$, and $M_- M_+ \simeq M_D^2$. Thus, in the regime $M_D \simeq 1$ GeV, we use the bound $0.3(p_F/M_D)^2\Theta_e^2\epsilon \lesssim 0.3$eV.

The above bound is displayed in Fig. 5 for comparison with the LFV constraints. LNV provides a subleading constraint within this particular inverse seesaw model, since the lepton number violating parameter is ϵ which is taken to be small compared to the other mass scales. However, as already emphasized above, more significant sensitivity to the mixing angle arises in the standard seesaw model, where we enlarge the Majorana terms in the mass matrix.

D. Electric dipole moments

Electric dipole moments (EDMs) constitute an important class of precision CP-odd observables. There are several channels by which CP violation can be communicated from the light NP degrees of freedom to the SM within a UV-complete model. CP-odd mediation can occur via the neutrino portal, and the phases in the Yukawa matrix Y_N, provided there are at least two singlet neutrinos N_i. The second channel is the Higgs portal. While obviously CP-even by itself, the scalar mediator can couple to a light NP sector in a manner that explicitly breaks CP, and this may be communicated to the SM via higher-order loop effects. We will first consider lepton EDMs induced through the neutrino portal before turning to more generic light NP mechanisms, and subsequently consider hadronic EDMs, which are distinct in that they can be generated at or close to the current level of sensitivity through the QCD θ-term.

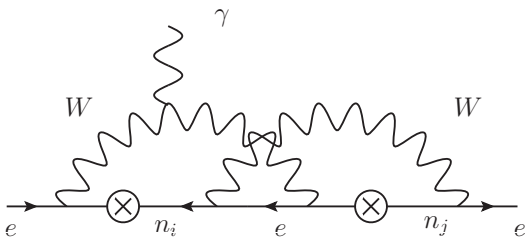

FIG. 6. An example of a W-loop diagram contributing to the lepton EDM. The crosses indicate neutrino mass insertions.

D.1. Paramagnetic (and leptonic) EDMs We first consider the same neutrino mass matrix studied in the previous subsection. In the SM extended with massive neutrinos, it is possible to generate an EDM at the two-loop level [70–72], an example of which is shown in Fig. 6. These diagrams can be shown to scale as

$$d_e \sim e m_e \left(\frac{G_F}{16\pi^2}\right)^2 \times \sum_{i<j} \Gamma_{ij} m_i m_j \frac{(m_j^2 - m_i^2)}{m_W^2} F\left(\frac{m_i}{m_W}, \frac{m_j}{m_W}, \frac{m_e}{m_W}\right), \tag{23}$$

where $\Gamma_{ij} = \mathrm{Im}\left\{(U_{ei}^*)^2 U_{ej}^2\right\}$, and $i, j = \nu, \pm$ are the neutrino mass eigenstates, and F is a loop function. Up to now, we have ignored the possible CP-odd phases in this model. However, in general not all the mass parameters are real. We choose to leave the physical CP-odd phase in $m_D = |m_D| e^{i\eta}$, and to ease the notation, replace $|m_D|$ simply with m_D. Given that the mixing angles are $m_D/M_D \lesssim 0.1$, we see that the contribution from the diagram with two internal light neutrinos will be tiny, $\mathcal{O}(m_{\nu_1} m_{\nu_2} \Delta m_{21}^2)$. Thus, we need only look at the cases where either one or two internal neutrinos are heavy, respectively called the $h-l$ or $h-h$ contributions. Looking at the $h-h$ contribution, the mixing that enters is Γ_{+-}, but both U_{e+}^2 and U_{e-}^2 have the same phase since they are controlled by m_D/M_D. The CP-odd phase thus cancels from the $h-h$ contribution. Next, the $h-l$ contribution is proportional to $\Gamma_{\nu_e \pm} \sim \pm m_D^2/(2M_D^2)\sin(2\eta)$, whereas $m_{\nu_e} M_\pm (M_\pm^2 - m_{\nu_e}^2) \sim m_D^2 M_D \epsilon \pm 3/2 m_D^2 \epsilon^2$. As a result, the $h-l$ contribution to the EDM vanishes at $\mathcal{O}(\epsilon)$. So at the lowest non-vanishing order, we have

$$d_e = d_e^{h-l} \sim \Theta_e^4 \frac{M_D^2}{m_W^2} \frac{\epsilon^2}{\Delta m_{21}^2} \cdot 10^{-53}\, \sin(2\eta) e\,\mathrm{cm}, \tag{24}$$

assuming the function $F\left(\frac{m_{\nu_e}}{m_W}, \frac{M_\pm}{m_W}, \frac{m_e}{m_W}\right)$ is of order unity. Within the allowed parameter space of Fig. 5, the above EDM is maximal for $\epsilon^2/\Delta m_{21}^2 \lesssim 10^{12}$, $M_D/m_W \sim 10^{-2}$ and $\Theta_e \lesssim 10^{-2}$, leading to an upper bound $d_e < 10^{-53} e \cdot \mathrm{cm}$. The suppression of the upper bound arises from the size of the Majorana mass term ϵ, which is set by the constraint on the active neutrino mass squared differences. Therefore, within this model it is not possible to generate a sizeable EDM. However, a far larger EDM is possible in a variant of this model with an extra visible-hidden Dirac mass coupling m_2. Namely, we switch gear and consider the following extended mass matrix,

$$-\mathcal{L}_\nu \supset (\nu_L \quad N_R \quad N_S) \begin{pmatrix} 0 & m_{D_1} & m_{D_2} \\ m_{D_1} & M_R & \epsilon \\ m_{D_2} & \epsilon & M_S \end{pmatrix} \begin{pmatrix} \nu_L \\ N_R \\ N_S \end{pmatrix}, \tag{25}$$

in the regime $M_{R,S} \gg m_{D_i}, \epsilon$. The limiting case $\epsilon = M_R = 0$ leads to two light neutrinos, and only one heavy neutrino, and will not lead to enhanced EDMs. Therefore we are forced to consider the full spectrum, and treating ϵ as a perturbation leads to

$$\begin{aligned} m_\nu &\approx m_\nu^0 + 2\frac{m_{D_1} m_{D_2}}{M_R M_S}\epsilon, \\ M_\pm &\approx M_\pm^0 \pm \frac{\epsilon}{\Delta M}\left(\epsilon + 2\frac{m_{D_1} m_{D_2}}{M_\pm}\right), \end{aligned} \tag{26}$$

where $m_\nu^0 \simeq (m_{D_1}^2 - m_{D_2}^2)/M$, $M_+^0 \simeq M_S$, $M_-^0 \simeq M_R$, $\Delta M = M_S - M_R$ is the Majorana mass splitting, and $M = (M_R + M_S)/2$ is the Majorana mass scale. Even though we are in a see-saw-like scenario with large Majorana masses, M_D easily evades the light neutrino mass constraints since they are now controlled by the fine tuning of $m_{D_2}^2 - m_{D_1}^2$. For simplicity we have ignored the phase in the mass eigenstates. As a consequence, to lowest order in $\epsilon(\sim 0)$ [71],

$$\begin{aligned} d_e &\sim e m_e \left(\frac{G_F}{16\pi^2}\right)^2 \frac{\Delta M}{M} \frac{m_{D_1}^2 m_{D_2}^2}{M^4} M^2 \\ &\quad \times \left(\frac{32}{3}\ln\left(\frac{M}{M_W}\right) - \frac{260}{9} + \frac{112}{27}\pi^2\right)\sin(2\eta), \\ &\sim \left(3 \cdot 10^{-35}\ e\,\mathrm{cm}\right) \frac{m_{D_1}^2 m_{D_2}^2}{M^4} \frac{M_S^2 - M_R^2}{\mathrm{GeV}^2} \sin(2\eta). \end{aligned} \tag{27}$$

The ratios $m_{D_i}/M \lesssim 10^{-1}$ are the visible-hidden mixing angles. Thus, on choosing a mass scale $M_S^2 - M_R^2 \sim M_S^2 \simeq 10^2\ \mathrm{GeV}^2$, one finds $d_e \lesssim 10^{-37} e \cdot \mathrm{cm}$. Allowing for significant fine tuning, it is possible to enhance this upper bound to $\sim 10^{-33} \mathrm{e} \cdot \mathrm{cm}$, which is still considerably lower than the current experimental upper limit $d_e < 8.7 \times 10^{-29} e \cdot \mathrm{cm}$ [73]. Therefore, we conclude that the sterile neutrino CP violating portal falls short of inducing d_e close to the current experimental bound.

Taking a more general approach, we now consider a more complex light hidden sector. We introduce a Dirac fermion ψ charged under $U(1)_V$ with CP-violating couplings to the scalar singlet S [74–79],

$$\mathcal{L}_{\mathrm{hid}}^{\mathrm{CP}} = \bar{\psi} i\gamma^\mu D_\mu^V \psi + \bar{\psi}(m_\psi + S(Y_S + i\tilde{Y}_S\gamma_5))\psi. \tag{28}$$

where $D_\mu^V = \partial_\mu - e' q_\psi V_\mu$. This hidden sector CP-violation can then be mediated to the SM via the CP-even vector and Higgs portals.

Loops of ψ can induce the CP-odd $SV\tilde{V}$ vertex shown in Fig. 7, which will contribute to EDMs at higher loop

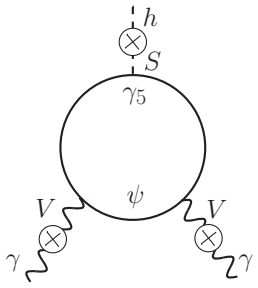

FIG. 7. The CP-odd $hF\tilde{F}$ vertex.

order, via e.g. Barr-Zee-type diagrams. For example, integrating out the scalar and one of the vector legs, one obtains a 'dark V-EDM' operator of the electron, which will in turn translate to the effective 'EDM radius' operator (analogous to the charge radius). Schematically, this process of integrating out short distance scales can be presented as

$$SV_{\mu\nu}\tilde{V}^{\mu\nu} \to \frac{i}{2}\bar{\psi}_e\sigma^{\mu\nu}\gamma_5\psi_e V_{\mu\nu} \to \frac{i}{2}\bar{\psi}_e\sigma^{\mu\nu}\gamma_5\psi_e\frac{\Box F_{\mu\nu}}{m_V^2}. \tag{29}$$

Denoting the coefficient in front of $\frac{i}{2}\bar{\psi}_e\sigma^{\mu\nu}\gamma_5\psi_e\Box F_{\mu\nu}$ as $r_{d_f}^2$, we can utilize existing EDM calculations. For simplicity, we assume that V is parametrically lighter than S and ψ, so the EDM radius takes the form (see e.g. [80])

$$r_{d_f}^2 = \frac{|e|\alpha'\tilde{Y}_S m_f}{16\pi^3 v m_\psi m_V^2}\kappa^2\sin(2\theta)\left[g(m_\psi^2/m_h^2) - g(m_\psi^2/m_S^2)\right], \tag{30}$$

where the loop function is given by

$$g(z) = \frac{z}{2}\int_0^1 dx \frac{1}{x(1-x)-z}\ln\left(\frac{x(1-x)}{z}\right), \tag{31}$$

and satisfies $g(1) \sim 1.17$, $g(z \ll 1) \sim z(\ln z)^2/2$ and $g(z \gg 1) \sim \frac{1}{2}\ln z$. Within the fully hierarchical regime,

$$m_V \ll m_S \ll m_\psi, \tag{32}$$

and taking $\theta \sim -Av/(m_h^2) \ll 1$, we have

$$r_{d_f}^2 = -\frac{|e|\alpha'\tilde{Y}_S m_f}{16\pi^3 v m_\psi m_V^2} \times \kappa^2\theta\ln(m_\psi^2/m_S^2). \tag{33}$$

This operator leads to the usual $s-p$ mixing of atomic orbitals, and the atomic EDM linked to the electron spin direction. While a full atomic calculation is required to deduce the size of the matrix element, we will resort to estimating its size by saturating $\Box$ with the square of the inverse radius of a K-shell. Then, the effective EDM radius translates to an electron EDM of size $d_e^{\rm eq} \sim (Z\alpha m_e)^2 r_{d_e}^2$, as long as $m_V > Z\alpha m_e$. Taking $m_V \sim (m_e\alpha Z)$, $q_\psi = 1$, $\alpha' = \alpha$, $\tilde{Y}_S = 1$ and taking the log to be $\mathcal{O}(1)$, we arrive at the estimate

$$d_e^{\rm eq} \sim 4\times 10^{-33}\ e\cdot{\rm cm}\times\left(\frac{1\,{\rm GeV}}{m_\psi}\right)\left(\frac{\kappa}{10^{-4}}\right)^2\left(\frac{\theta}{10^{-3}}\right), \tag{34}$$

which is still well below the current sensitivity to the electron EDM [73]. The main difficulty is in taking m_V in the sub-MeV range, where $g-2$ of the electron imposes a strong limit on kinetic mixing, $\kappa < 10^{-4}$. We note in passing that extracting a proper limit on the 'dark V-EDM', or $r_{d_e}^2$, is a well-motivated problem for atomic physics, in line with the recent investigation of CP-odd operators induced by a mediator of mass comparable to the inverse atomic scale [81].

Another contribution to the experimentally accessible paramagnetic EDMs of atoms and molecules is the semi-leptonic interaction $C_S\bar{N}N\bar{e}i\gamma_5 e$. This operator can also be generated through the $hV\tilde{V}$ vertex, and allows access to a regime with larger m_V for which the constraints on κ are somewhat weaker. However, this contribution is still not at a level that can approach the current experimental sensitivity. Thus, at least within this restricted class of hidden sectors, we conclude that paramagnetic EDMs (and specifically lepton EDMs) are in practice a probe of UV new physics.

D.2. Diamagnetic (and hadronic) EDMs Hadronic EDMs can also be induced using the mechanism outlined above, via the hidden sector Barr-Zee diagram, although again necessarily below the current level of sensitivity. However, hadronic EDMs can also be generated by the QCD θ-term, which is a marginal operator [82–85]. The strongest current limits in this sector are from the EDM of the neutron [86]

$$|d_n| < 2.9\times 10^{-26} e\,{\rm cm}, \tag{35}$$

and the EDM of the Hg atom [87],

$$|d_{Hg}| < 3.1\times 10^{-29} e\,{\rm cm}, \tag{36}$$

where the apparent strength of the Hg EDM bound is tempered by Schiff screening of the nuclear EDM. The contribution of $\bar{\theta}$ to the neutron EDM takes the form (see e.g. [88]),

$$d_n(\bar{\theta}) \sim 3\times 10^{-26}\left(\frac{\bar{\theta}}{10^{-10}}\right) e{\rm cm}. \tag{37}$$

This leads to the current constraint of $\bar{\theta} < 10^{-10}$. The contribution of $\bar{\theta}$ to d_{Hg} is more complex, and for some time it appeared that it would be isospin-suppressed, with the Schiff moment for Hg primarily sensitive to the CP-odd isovector pion-nucleon coupling $\bar{g}^1(\bar{\theta}) \sim 0.001\bar{\theta}$ rather than the isoscalar coupling $\bar{g}^0(\bar{\theta}) \sim 0.05\bar{\theta}$. However, more recent analyses of the Hg Schiff moment have indicated that $\bar{g}^0$ may provide a comparable contribution to $\bar{g}^1$ [89]. Taking the current 'best values' [5] indicates that

$$d_{Hg}(\bar{\theta}) \sim 5\times 10^{-30}\left(\frac{\bar{g}^0(\bar{\theta})}{0.05\times 10^{-10}} + \mathcal{O}(\bar{g}^1(\bar{\theta}))\right) e{\rm cm}. \tag{38}$$

This is a factor of 6 below the current bound, but given that the precision of the calculation is generally understood to be at the order of magnitude level [5, 88], it

is clear that a nonzero detection of d_{Hg} could not unambiguously be distinguished from the effect of nonzero $\bar{\theta}$.

We conclude that, at current levels of sensitivity, nonzero detections of the dominant hadronic EDM observables could be explained without additional UV new physics, simply through CP-odd QCD physics in the form of $\bar{\theta}$. Further improvements in the sensitivity to d_n could of course change this picture.

E. Hadronic flavor violation

We now turn to precision quark flavor-violating observables, with the $b \to s\gamma$ transition as a benchmark. There are a couple of features which clearly distinguish these observables, particularly concerning the role of light new physics. Firstly, since the RH states are charged, there is no analogue of the neutrino portal, and thus no renormalizable flavor-violating interactions that do not involve new charged states. Given the existing limits on new light degrees of freedom which are charged, this pushes hadronic flavor violating observables into a category that is primarily sensitive to UV new physics. Having said this, the second distinguishing feature is that the SM itself provides non-negligible contributions to hadronic flavor violation through the CKM matrix. This allows for new flavor violating transitions to occur on introducing purely flavor-diagonal light NP. An example is the kinetic mixing between V and γ (or Z) in (3) that can induce flavor-violating transitions of the form $b \to sV$ and thus $b \to s\gamma^*(Z^*)$. However, given the constraints on kinetic mixing, this mechanism is too weak to produce sizeable effects without additional $V - Z$ mass mixing that in turn requires new UV physics [90]. Moreover, utilizing a W-boson loop at leading order for example, the SM contributes to $\mathrm{Br}(\bar{B} \to X_s\gamma) = (3.60 \pm 0.30) \cdot 10^{-4}$ [91], while the BaBar sensitivity is $\mathrm{Br}(\bar{B} \to X_s\gamma) \simeq (3.15 \pm 0.23) \cdot 10^{-4}$ [92]. Thus, the sensitivity to new physics is also limited by the precision of SM calculations.

Since these observables are not primarily sensitive to light new physics in the categories that we have delineated, we will not consider them in detail. However, it is worth outlining how a model with low energy flavor violation can be realized, albeit one that still relies on additional heavy charged states for consistency. We consider a model in which we gauge an anomaly-free $U(1)'$ combination of quark flavors, $Q_{f1} - Q_{f2}$ [93, 94], with a diagonal (and vectorial) gauge coupling of the form [95–98],

$$\mathcal{L}_{Z'} = g_z Z'_\mu \sum_{q=Q_f,u_f,d_f} z_f \bar{q}\gamma^\mu q, \tag{39}$$

with e.g. $z_{Q_3} = z_b = -z_{Q_2} = -z_s = 1$. On transforming to the mass eigenstate basis, this non-universal coupling will generate a flavor-violating $b - s - Z'$ vertex, and mediate sizable flavor violating transitions. In practice, this imposes significant constraints on the combinations of $g_z z_{Q,b,s}$, and is usually used to motivate flavor-universal $U(1)'$ charge assignments. Here, we are interested in having a light Z' that can indeed mediate these transitions at the level to which current experiments are sensitive. If we assign integer charges, then a small gauge coupling $g_z \sim 10^{-5}$ will be sufficient for this purpose. As has recently been emphasized [94], $K^0 - \bar{K}^0$ mixing requires $g_z|z_{Q_2} - z_{Q_1}| < 10^{-5} M_{Z'}/(1\,\mathrm{GeV})$, while $B^0 - \bar{B}^0$ mixing imposes similar constraints on $g_z|z_{Q_3} - z_{Q_1}|$. An explicit Z' model based on 'horizontal' flavor symmetries, related to possible anomalies in B^0 decays, can be found in [99].

The gauging of flavor non-universal symmetries leads to further model building requirements for the quark mass spectrum, as the Yukawa matrices are now subject to additional constraints. Additional charged Higgs fields are required, which necessarily lie above the EW scale given the current LHC constraints. Thus, while quark flavor-violation could be mediated via a light Z', the model would necessarily involve charged states above the EW scale, and thus UV new physics.

F. Baryon number violation

New non-SM sources of baryon number violation, for which the primary precision experiments are searches for proton decay, necessarily require new UV physics. The minimal baryonic vertex that converts two quarks into an anti-quark and a lepton corresponds to a higher-dimensional operator that *requires* new charged states in any UV completion of which we are aware. Therefore any detection of proton decay or $n - \bar{n}$ oscillation will most likely point to the weak scale or above, as a possible source of baryon number violation. An alternative means of introducing a low energy mediation mechanism is to gauge B (see e.g. [100]) within a more extended gauge group, and rely on a new non-perturbative sector to break this new gauge symmetry. This, however, may not necessarily lead to any proton decay, or any other baryon number-violating observable without the participation of new charged fields in the UV.

4. CONCLUSIONS

Empirical evidence for new physics, e.g. neutrino oscillations or dark matter, does not always provide us with much guidance as to a natural mass or energy scale. As noted in the Introduction, there are UV and IR scenarios for neutrino oscillations, both of which are currently viable. Sometimes it is argued that the evidence for dark matter points to NP at a UV scale at or above the electroweak scale (i.e. via the 'WIMP miracle'). While this may be true for examples such as the MSSM neutralino or the QCD axion, which require UV completion with states above the EW scale, there are many viable examples of dark matter based on UV complete models that do

not introduce additional heavy degrees of freedom: these include keV-scale sterile neutrinos, and light scalar and vector fields that are populated via the freeze-in mechanism and/or vacuum misalignment (see *e.g.* [101–103] for some early ideas). Therefore, the existence of dark matter cannot unambiguously be used as a pointer to new UV physics, any more than the existence of neutrino mass can be used in the same way. This may change if, for example, very energetic products of dark matter annihilation or decay are discovered that would be hard to accommodate within the light NP paradigm. Nonetheless, the observation that various scenarios currently remain open and experimentally testable has motivated the analysis in this paper, namely surveying the possible implications of light NP for precision measurements.

We have explored the sensitivity of several classes of precision observables to UV-complete models of light NP. While it is common to automatically interpret precision measurements in terms of generic UV new physics scenarios, we have emphasized that many of these observables are often most simply considered within models of weakly-coupled hidden sectors. Operationally, the measurement of any deviation from a SM prediction will necessarily lead to a lengthy process to uncover its origin. Even conclusive evidence for a new phenomenon (neutrino oscillation, dark matter) still entails further work to discriminate between viable interpretations involving light NP and physics at the EW scale and above. Currently, this process is underway for the measurement of $g-2$ for muons, where both light NP and EW scale phenomena may in principle be causing the discrepancy with SM predictions. Another existing hint of a deviation, in hadronic flavor physics (semileptonic B decays at LHCb), points instead to models of NP which necessarily involve new degrees of freedom at the EW scale or above. The exercise performed in this paper generalizes these examples to a broader set of precision observables and broader classes of models for light NP. In particular, we have found that the neutrino portal allows for a description of many observables in the leptonic sector, while observation of a nonzero electron EDM or related leptonic CP-violating observables would point to NP at or above the electroweak scale. In addition, we observed that several classes of observables that intrinsically involve hadronic flavor violation, baryon number violation, or changes to the charged currents (and thus electroweak symmetry breaking), seemingly allow an unambiguous interpretation in term of new short-distance physics.

ACKNOWLEDGMENTS

The work of M.L., M.P. and A.R. is supported in part by NSERC, Canada, and research at the Perimeter Institute is supported in part by the Government of Canada through NSERC and by the Province of Ontario through MEDT.

[1] G. Aad *et al.* (ATLAS Collaboration), Phys.Lett. **B716**, 1 (2012), arXiv:1207.7214 [hep-ex].
[2] S. Chatrchyan *et al.* (CMS Collaboration), Phys.Lett. **B716**, 30 (2012), arXiv:1207.7235 [hep-ex].
[3] M. Raidal, A. van der Schaaf, I. Bigi, M. Mangano, Y. K. Semertzidis, *et al.*, Eur.Phys.J. **C57**, 13 (2008), arXiv:0801.1826 [hep-ph].
[4] M. Pospelov and A. Ritz, Annals Phys. **318**, 119 (2005), arXiv:hep-ph/0504231 [hep-ph].
[5] J. Engel, M. J. Ramsey-Musolf, and U. van Kolck, Prog.Part.Nucl.Phys. **71**, 21 (2013), arXiv:1303.2371 [nucl-th].
[6] A. de Gouvea and P. Vogel, Prog.Part.Nucl.Phys. **71**, 75 (2013), arXiv:1303.4097 [hep-ph].
[7] O. Gedalia and G. Perez, (2010), arXiv:1005.3106 [hep-ph].
[8] Z. Maki, M. Nakagawa, and S. Sakata, Prog.Theor.Phys. **28**, 870 (1962).
[9] B. Pontecorvo, Sov.Phys.JETP **26**, 984 (1968).
[10] S. Weinberg, Phys.Rev.Lett. **43**, 1566 (1979).
[11] T. Asaka, S. Blanchet, and M. Shaposhnikov, Phys.Lett. **B631**, 151 (2005), arXiv:hep-ph/0503065 [hep-ph].
[12] E. K. Akhmedov, V. Rubakov, and A. Y. Smirnov, Phys.Rev.Lett. **81**, 1359 (1998), arXiv:hep-ph/9803255 [hep-ph].
[13] T. Asaka and M. Shaposhnikov, Phys.Lett. **B620**, 17 (2005), arXiv:hep-ph/0505013 [hep-ph].
[14] K. Petraki and A. Kusenko, Phys.Rev. **D77**, 065014 (2008), arXiv:0711.4646 [hep-ph].
[15] A. de Gouvea, Phys.Rev. **D72**, 033005 (2005), arXiv:hep-ph/0501039 [hep-ph].
[16] A. Kusenko, Phys.Rept. **481**, 1 (2009), arXiv:0906.2968 [hep-ph].
[17] S. Weinberg, Phys.Rev. **D22**, 1694 (1980); H. Weldon and A. Zee, Nucl.Phys. **B173**, 269 (1980); W. Buchmuller and D. Wyler, Nucl.Phys. **B268**, 621 (1986); K. Babu and C. N. Leung, Nucl.Phys. **B619**, 667 (2001), arXiv:hep-ph/0106054 [hep-ph]; A. de Gouvea and J. Jenkins, Phys.Rev. **D77**, 013008 (2008), arXiv:0708.1344 [hep-ph]; F. Bonnet, D. Hernandez, T. Ota, and W. Winter, JHEP **0910**, 076 (2009), arXiv:0907.3143 [hep-ph]; B. Grzadkowski, M. Iskrzynski, M. Misiak, and J. Rosiek, JHEP **1010**, 085 (2010), arXiv:1008.4884 [hep-ph]; F. del Aguila, A. Aparici, S. Bhattacharya, A. Santamaria, and J. Wudka, JHEP **1206**, 146 (2012), arXiv:1204.5986 [hep-ph]; P. W. Angel, N. L. Rodd, and R. R. Volkas, Phys.Rev. **D87**, 073007 (2013), arXiv:1212.6111 [hep-ph]; K. Babu and R. Mohapatra, Phys.Rev.Lett. **109**, 091803 (2012), arXiv:1207.5771 [hep-ph]; Phys.Rev. **D86**, 035018 (2012), arXiv:1203.5544 [hep-ph]; G. Chalons and F. Domingo, Phys.Rev. **D89**, 034004 (2014), arXiv:1303.6515 [hep-ph]; L. Lehman, Phys.Rev. **D90**, 125023 (2014), arXiv:1410.4193 [hep-ph].
[18] R. Essig, J. A. Jaros, W. Wester, P. H. Adrian, S. An-

dreas, *et al.*, (2013), arXiv:1311.0029 [hep-ph].
[19] J. Preskill, Annals Phys. **210**, 323 (1991).
[20] B. Batell, S. Jung, and C. E. Wagner, JHEP **1312**, 075 (2013), arXiv:1309.2297 [hep-ph].
[21] B. Holdom, Phys.Lett. **B166**, 196 (1986); R. Foot and X.-G. He, Phys.Lett. **B267**, 509 (1991); R. Foot, H. Lew, and R. Volkas, Phys.Lett. **B272**, 67 (1991); M. Pospelov, A. Ritz, and M. B. Voloshin, Phys.Lett. **B662**, 53 (2008), arXiv:0711.4866 [hep-ph]; B. Batell, M. Pospelov, and A. Ritz, Phys.Rev. **D80**, 095024 (2009), arXiv:0906.5614 [hep-ph].
[22] B. C. Odom, D. Hanneke, B. D'Urso, and G. Gabrielse, Phys.Rev.Lett. **97**, 030801 (2006).
[23] G. Bennett *et al.* (Muon G-2 Collaboration), Phys.Rev. **D73**, 072003 (2006), arXiv:hep-ex/0602035 [hep-ex].
[24] H. Davoudiasl, H.-S. Lee, and W. J. Marciano, Phys.Rev. **D86**, 095009 (2012), arXiv:1208.2973 [hep-ph].
[25] A. Czarnecki and W. J. Marciano, Phys.Rev. **D64**, 013014 (2001), arXiv:hep-ph/0102122 [hep-ph].
[26] M. Pospelov, Phys.Rev. **D80**, 095002 (2009), arXiv:0811.1030 [hep-ph].
[27] P. Fayet, Phys.Rev. **D75**, 115017 (2007), arXiv:hep-ph/0702176 [HEP-PH].
[28] S. Gninenko and N. Krasnikov, Phys.Lett. **B513**, 119 (2001), arXiv:hep-ph/0102222 [hep-ph].
[29] J. Lees *et al.* (BaBar Collaboration), Phys.Rev.Lett. **113**, 201801 (2014), arXiv:1406.2980 [hep-ex].
[30] E. Goudzovski (NA48/2 Collaboration), (2014), arXiv:1412.8053 [hep-ex].
[31] B. Batell, P. deNiverville, D. McKeen, M. Pospelov, and A. Ritz, Phys.Rev. **D90**, 115014 (2014), arXiv:1405.7049 [hep-ph].
[32] B. Batell, R. Essig, and Z. Surujon, Phys.Rev.Lett. **113**, 171802 (2014), arXiv:1406.2698 [hep-ph].
[33] Y. Kahn, G. Krnjaic, J. Thaler, and M. Toups, (2014), arXiv:1411.1055 [hep-ph].
[34] W. Altmannshofer, S. Gori, M. Pospelov, and I. Yavin, Phys.Rev.Lett. **113**, 091801 (2014), arXiv:1406.2332 [hep-ph].
[35] W. Altmannshofer, S. Gori, M. Pospelov, and I. Yavin, Phys.Rev. **D89**, 095033 (2014), arXiv:1403.1269 [hep-ph].
[36] R. N. Mohapatra and J. W. F. Valle, *Proceedings, 23RD International Conference on High Energy Physics, JULY 16-23, 1986, Berkeley, CA*, Phys. Rev. **D34**, 1642 (1986); R. N. Mohapatra, Phys. Rev. Lett. **56**, 561 (1986); M. Gonzalez-Garcia and J. Valle, Phys.Lett. **B216**, 360 (1989); S. Fraser, E. Ma, and O. Popov, Phys.Lett. **B737**, 280 (2014), arXiv:1408.4785 [hep-ph].
[37] F. F. Deppisch, P. S. B. Dev, and A. Pilaftsis, (2015), arXiv:1502.06541 [hep-ph].
[38] M. Brooks *et al.* (MEGA Collaboration), Phys.Rev.Lett. **83**, 1521 (1999), arXiv:hep-ex/9905013 [hep-ex].
[39] J. Adam *et al.* (MEG Collaboration), Phys.Rev.Lett. **110**, 201801 (2013), arXiv:1303.0754 [hep-ex].
[40] F. Renga (The MEG Collaboration), (2014), arXiv:1410.4705 [hep-ex].
[41] T. Cheng and L.-F. Li, Phys.Rev.Lett. **38**, 381 (1977).
[42] J. Bjorken, K. D. Lane, and S. Weinberg, Phys.Rev. **D16**, 1474 (1977).
[43] E. Ma and A. Pramudita, Phys.Rev. **D24**, 1410 (1981).
[44] J. Casas and A. Ibarra, Nucl.Phys. **B618**, 171 (2001), arXiv:hep-ph/0103065 [hep-ph].
[45] A. Ilakovac and A. Pilaftsis, Nucl.Phys. **B437**, 491 (1995), arXiv:hep-ph/9403398 [hep-ph].
[46] B. Grinstein, (2015), arXiv:1501.05283 [hep-ph].
[47] J. Vergados, Phys.Rept. **133**, 1 (1986).
[48] T. Kosmas, G. Leontaris, and J. Vergados, Prog.Part.Nucl.Phys. **33**, 397 (1994), arXiv:hep-ph/9312217 [hep-ph].
[49] S. Weinberg and G. Feinberg, Phys.Rev.Lett. **3**, 111 (1959).
[50] T. Donnelly and J. Walecka, Ann.Rev.Nucl.Part.Sci. **25**, 329 (1975).
[51] W. H. Bertl *et al.* (SINDRUM II Collaboration), Eur.Phys.J. **C47**, 337 (2006).
[52] H. Natori (DeeMe), Nucl.Phys.Proc.Suppl. **248-250**, 52 (2014).
[53] R. K. Kutschke, (2011), arXiv:1112.0242 [hep-ex].
[54] A. Lusiani, PoS **KAON**, 054 (2008), arXiv:0709.1599 [hep-ex].
[55] A. Pich, NATO Sci.Ser.B **363**, 173 (1997), arXiv:hep-ph/9701263 [hep-ph].
[56] B. Aubert *et al.* (BaBar Collaboration), Phys.Rev.Lett. **105**, 051602 (2010), arXiv:0912.0242 [hep-ex].
[57] C. Dib, J. C. Helo, M. Hirsch, S. Kovalenko, and I. Schmidt, Phys.Rev. **D85**, 011301 (2012), arXiv:1110.5400 [hep-ph].
[58] A. Abada, A. Teixeira, A. Vicente, and C. Weiland, JHEP **1402**, 091 (2014), arXiv:1311.2830 [hep-ph].
[59] F. Bergsma *et al.* (CHARM), Phys.Lett. **B166**, 473 (1986).
[60] H. Klapdor-Kleingrothaus and I. Krivosheina, Mod.Phys.Lett. **A21**, 1547 (2006).
[61] A. Bakalyarov, A. Y. Balysh, S. Belyaev, V. Lebedev, and S. Zhukov (C03-06-23.1), Phys.Part.Nucl.Lett. **2**, 77 (2005), arXiv:hep-ex/0309016 [hep-ex].
[62] A. Gando *et al.* (KamLAND-Zen Collaboration), Phys.Rev.Lett. **110**, 062502 (2013), arXiv:1211.3863 [hep-ex].
[63] M. Auger *et al.* (EXO Collaboration), Phys.Rev.Lett. **109**, 032505 (2012), arXiv:1205.5608 [hep-ex].
[64] A. Garfagnini, (2014), arXiv:1408.2455 [hep-ex].
[65] D. Palioselitis (GERDA), J.Phys.Conf.Ser. **606**, 012006 (2015).
[66] B. Schwingenheuer, Annalen Phys. **525**, 269 (2013), arXiv:1210.7432 [hep-ex].
[67] P. Bhupal Dev, S. Goswami, M. Mitra, and W. Rodejohann, Phys.Rev. **D88**, 091301 (2013), arXiv:1305.0056 [hep-ph].
[68] P. Bamert, C. Burgess, and R. Mohapatra, Nucl.Phys. **B438**, 3 (1995), arXiv:hep-ph/9408367 [hep-ph].
[69] A. Faessler, M. Gonzalez, S. Kovalenko, and F. Simkovic, (2014), arXiv:1408.6077 [hep-ph].
[70] D. Ng and J. N. Ng, Mod.Phys.Lett. **A11**, 211 (1996), arXiv:hep-ph/9510306 [hep-ph].
[71] J. P. Archambault, A. Czarnecki, and M. Pospelov, Phys.Rev. **D70**, 073006 (2004), arXiv:hep-ph/0406089 [hep-ph].
[72] A. de Gouvea and S. Gopalakrishna, Phys.Rev. **D72**, 093008 (2005), arXiv:hep-ph/0508148 [hep-ph].
[73] J. Baron *et al.* (ACME Collaboration), Science **343**, 269 (2014), arXiv:1310.7534 [physics.atom-ph].
[74] C. Bird, R. V. Kowalewski, and M. Pospelov, Mod.Phys.Lett. **A21**, 457 (2006), arXiv:hep-ph/0601090 [hep-ph].

[75] D. O'Connell, M. J. Ramsey-Musolf, and M. B. Wise, Phys.Rev. **D75**, 037701 (2007), arXiv:hep-ph/0611014 [hep-ph].

[76] V. Barger, P. Langacker, M. McCaskey, M. J. Ramsey-Musolf, and G. Shaughnessy, Phys.Rev. **D77**, 035005 (2008), arXiv:0706.4311 [hep-ph].

[77] R. Sato, S. Shirai, and T. T. Yanagida, Phys.Lett. **B704**, 490 (2011), arXiv:1105.0399 [hep-ph].

[78] P. J. Fox, D. Tucker-Smith, and N. Weiner, JHEP **1106**, 127 (2011), arXiv:1104.5450 [hep-ph].

[79] I. Low, J. Lykken, and G. Shaughnessy, Phys.Rev. **D84**, 035027 (2011), arXiv:1105.4587 [hep-ph].

[80] D. McKeen, M. Pospelov, and A. Ritz, Phys.Rev. **D86**, 113004 (2012), arXiv:1208.4597 [hep-ph].

[81] H. Gharibnejad and A. Derevianko, Phys.Rev. **D91**, 035007 (2015), arXiv:1411.6077 [physics.atom-ph].

[82] V. Baluni, Phys.Rev. **D19**, 2227 (1979).

[83] R. Crewther, P. Di Vecchia, G. Veneziano, and E. Witten, Phys.Lett. **B88**, 123 (1979).

[84] M. Pospelov and A. Ritz, Phys.Rev. **D63**, 073015 (2001), arXiv:hep-ph/0010037 [hep-ph].

[85] M. Pospelov and A. Ritz, Phys.Rev.Lett. **83**, 2526 (1999), arXiv:hep-ph/9904483 [hep-ph].

[86] C. Baker, D. Doyle, P. Geltenbort, K. Green, M. van der Grinten, *et al.*, Phys.Rev.Lett. **97**, 131801 (2006), arXiv:hep-ex/0602020 [hep-ex].

[87] W. Griffith, M. Swallows, T. Loftus, M. Romalis, B. Heckel, *et al.*, Phys.Rev.Lett. **102**, 101601 (2009).

[88] M. Pospelov and A. Ritz, Annals Phys. **318**, 119 (2005), arXiv:hep-ph/0504231 [hep-ph].

[89] S. Ban, J. Dobaczewski, J. Engel, and A. Shukla, Phys.Rev. **C82**, 015501 (2010), arXiv:1003.2598 [nucl-th].

[90] H. Davoudiasl, H.-S. Lee, and W. J. Marciano, Phys.Rev. **D85**, 115019 (2012), arXiv:1203.2947 [hep-ph].

[91] P. Gambino and M. Misiak, Nucl.Phys. **B611**, 338 (2001), arXiv:hep-ph/0104034 [hep-ph].

[92] J. Lees *et al.* (BaBar Collaboration), Phys.Rev. **D86**, 052012 (2012), arXiv:1207.2520 [hep-ex].

[93] P. Batra, B. A. Dobrescu, and D. Spivak, J.Math.Phys. **47**, 082301 (2006), arXiv:hep-ph/0510181 [hep-ph].

[94] B. A. Dobrescu and C. Frugiuele, Phys.Rev.Lett. **113**, 061801 (2014), arXiv:1404.3947 [hep-ph].

[95] Y. Nir and D. J. Silverman, Phys.Rev. **D42**, 1477 (1990).

[96] P. Langacker and M. Plumacher, Phys.Rev. **D62**, 013006 (2000), arXiv:hep-ph/0001204 [hep-ph].

[97] M. S. Carena, A. Daleo, B. A. Dobrescu, and T. M. Tait, Phys.Rev. **D70**, 093009 (2004), arXiv:hep-ph/0408098 [hep-ph].

[98] E. Salvioni, A. Strumia, G. Villadoro, and F. Zwirner, JHEP **1003**, 010 (2010), arXiv:0911.1450 [hep-ph].

[99] A. Crivellin, G. DAmbrosio, and J. Heeck, Phys.Rev. **D91**, 075006 (2015), arXiv:1503.03477 [hep-ph].

[100] P. Fileviez Perez and M. B. Wise, Phys.Rev. **D82**, 011901 (2010), arXiv:1002.1754 [hep-ph].

[101] S. Dodelson and L. M. Widrow, Phys.Rev.Lett. **72**, 17 (1994), arXiv:hep-ph/9303287 [hep-ph].

[102] J. McDonald, Phys.Rev.Lett. **88**, 091304 (2002), arXiv:hep-ph/0106249 [hep-ph].

[103] F. Piazza and M. Pospelov, Phys.Rev. **D82**, 043533 (2010), arXiv:1003.2313 [hep-ph].